JOURNAL OF PROPULSION AND POWER
Vol. 16, No. 6, November–December 2000

Development of the Low-Power Xenon Ion Thruster for Lightweight Satellites

O. A. Gorshkov*
Keldysh Research Center, 125438, Moscow, Russia
V. G. Grigor'yan†
Moscow Aviation Institute, 125871, Moscow, Russia
and
V. A. Muravlev‡
Keldysh Research Center, 125438, Moscow, Russia

Results are described of an experimental study examining the laboratory model of the 5-cm xenon ion thruster with power in the range from 50 to 100 W. The investigation was aimed at the study of the efficiency of the small-size thruster discharge chamber operating in combination with two grid systems of different types at a low-power consumption. A beam ion production cost between 260–370 W/A at a propellant utilization efficiency ranging from 0.77 to 0.81 was realized in experiments conducted with the laboratory model. The use of the string grid system with small elementary cell sizes and large transparency for ions is shown to reduce substantially the accelerator grid potential compared to the conventional flat grid system.

Nomenclature

C_i = beam ion production cost
e = electron charge
g = free fall acceleration
I_b = ion beam current
I_d = discharge current
M = ion mass
$\dot{m}$ = propellant flow rate
N = total power
R = thrust
R_{sp} = specific impulse
U_a = accelerator grid potential
U_d = discharge voltage
U_s = screen grid potential
η_e = electrical efficiency
η_g = propellant utilization efficiency
η_t = thrust efficiency

Introduction

INTENSIVE activity toward development and use of next-generation small-size spacecraft for various purposes (on-line communications, remote Earth sensing, scientific study, etc.) will greatly reduce a space program's cost. The orbit correction propulsion systems on these small spacecraft may use ion thrusters with capabilities to operate at a low-power consumption (less than 100 W) with a high specific impulse (3000 s and higher).

Tentative analysis of propulsion system requirements of small-size spacecraft (as to a level of thrust and total impulse, specific impulse, and power consumption) showed that the ion propulsion systems may be used for keeping the small-size spacecraft relative positioning, drag compensation, low-orbit spacecraft braking, and orbit correction to provide necessary conditions for space survey.[1,2]

There are several publications concerning thrusters of a size range of 5–8 cm, but for the most part, these dealt with mercury ion thrusters.[3,4] The test results of the 5-cm-diam xenon thruster are presented in Ref. 5. Operation of the thruster was studied at a power less than 100 W. A beam ion production cost between 300 and 400 W/A was realized at a propellant utilization efficiency from 0.65 to 0.75.

The ion thruster performance is determined by the operating characteristics of the major assemblies: cathode assembly, discharge chamber, and grid system. Operation of these assemblies integral with the small-size ion thruster requires special accuracy because the ratio of the volume in which ions are being generated to the area of construction members where charged particles are recombinating is decreased when compared to large-size ion thrusters.

This paper describes experiments conducted to investigate the laboratory model of the 5-cm xenon ion thruster with a power of 50–100 W and presents the results obtained. The objective was to carry out a preliminary study of the laboratory model efficiency with different grid systems.

Laboratory-Model Ion Thruster

Experimental results of the laboratory-model ion thruster with a 52-mm-diam anode are described. The thruster is based on Kaufman-type configuration.[6] The thruster discharge chamber (Fig. 1) is formed by the cylindrical shell, whose diameter and length equal 60 mm, installed between the backplate and the mount ring of the screen grid. The 52-mm-diam anode is attached to the shell via insulators. Within the discharge chamber, the two-pole magnetic system produces the divergent magnetic field with a magnetic induction of about 10^{-2} T, excited by the six solenoids situated on the outside of the shell. The cathode assembly based on the capillary hollow cathode using emitting material LaB_6 is placed within the cathode polepiece. The xenon propellant is fed to the discharge chamber via the two channels: through the hollow cathode and the flow distributor on the back wall of the discharge chamber.

Two types of grid systems were examined during the thruster's operation. In the first case, the conventional beam-extraction system was used: Its screen and accelerator grids are made in the form of molybdenum perforated plates. In the second case, the screen and accelerator grids were formed by the strings fastened on the mount rings via spring elements. The grid system schemes with the basic dimensions are shown in Fig. 2. In both configurations, the ring enclosing the whole beam was used as a decelerator electrode.

Received 19 March 1997; revision received 1 June 1998; accepted for publication 10 December 1999.

*Chief, Department for Electrophysics.
†Professor, Department of Electric Propulsion and Space Vehicles Power Plants.
‡Senior Scientific Worker, Department of Electrophysics.

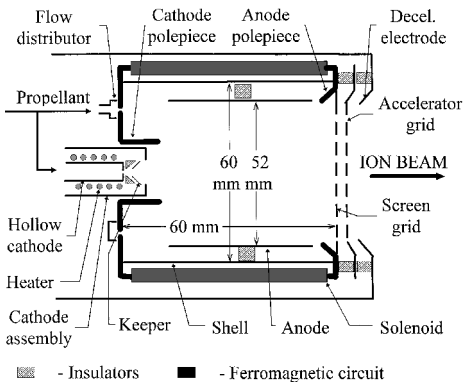

Fig. 1 Scheme of the laboratory-model ion thruster.

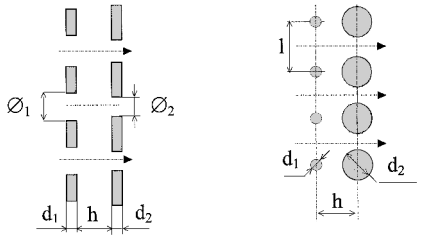

Flat grids **String grids**

$d_1=d_2=1$ mm; h=1 mm $d_1=0.2$ mm; $d_2=0.9$ mm;

$\varnothing_1=4.3$ mm; $\varnothing_2=2.5$ mm l= 1.5 mm; h=1.4 mm

Fig. 2 Scheme of grid systems used in the experiments.

Experimental Results

The laboratory-model tests were conducted in the test facility including 1.2-m^3-volume vacuum chamber (Fig. 3). The chamber was pumped by turbomolecular pumps. Pressure was checked by the ionization gauge installed on the chamber wall at a level of the thruster exit section. It ranged from 10^{-3} Pa in the flow-free mode to 5×10^{-3} Pa with an operating thruster.

To estimate performance parameters of the laboratory-model ion thruster the following relationships were used:

$$\eta_g = \frac{I_b}{\dot{m}}, \qquad C_i = \frac{U_d\cdot(I_d - I_b)}{I_b}$$

$$\eta_e = \frac{I_b\cdot(U_s + U_d)}{I_b\cdot U_s + I_d\cdot U_d}, \qquad \eta_t = \eta_e\cdot\eta_g$$

$$R = I_b\cdot\sqrt{\frac{2U_s\cdot M}{e}}, \qquad R_{sp} = \frac{R}{\dot{m}\cdot g}$$

The precision of measurement of the flow rate (±5%) and the discharge current (±4%) are responsible for major errors in the experiment. The error of the performance parameters calculated does not exceed ±6%.

These relations do not account for losses caused by the presence of doubly charged ions in the beam. Wilbur and Kaufman[7] showed that fraction losses amount to about 6% at $U_d \approx 45$ V for xenon. Hence, the error stemming from the presence of doubly charged ions does not exceed 6% for calculating thrust, specific impulse, propellant utilization efficiency, and thrust efficiency from the preceding formulas.

First, the grid system with flat grids manufactured of 1-mm thick molybdenum was installed into the ion thruster. Holes in the screen grid had a 4.3 mm diameter and in the accelerator grid a 2.5 mm diameter. The transparencies (open-area to total-area ratios) of grids were 0.58 and 0.17, respectively. Shown in Fig. 4 is the beam ion production cost as a function of propellant utilization efficiency at a beam current from 30 to 35 mA that was obtained by use of this grid

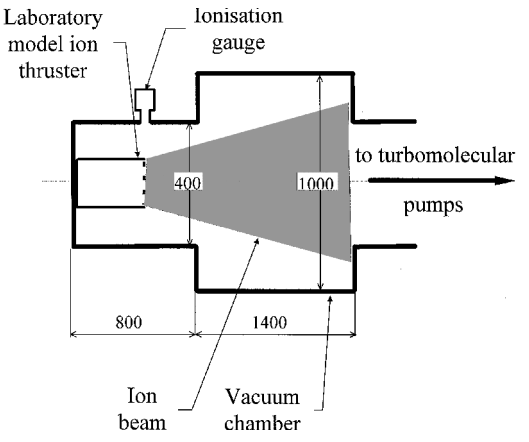

Fig. 3 Scheme of the test facility.

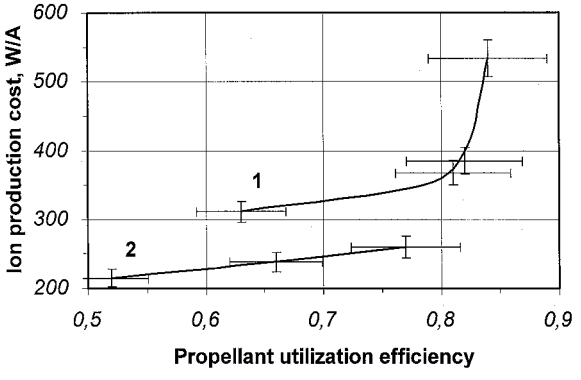

Fig. 4 Experimental values of the ion production cost as a function of the propellant utilization efficiency for two types of grid systems: flat grids U_s = 1200 V, U_a = − 1050 V, and I_b = 32 mA (1) and string grids U_s = 1000 V, U_a = − 300 V, and I_b = 30 mA (2).

system (the upper curve). The screen grid potential was 1200 V, and the accelerator grid potential −1050 V.

The propellant flow rate was decreased from 50 to 30 eq. mA, and all of the gas was fed through the hollow cathode. The discharge voltage changed from 38 to 50 V. Figure 4 shows that in the region of reasonable tradeoff between power consumption and propellant losses the ion production cost is 370 W/A at $\eta_g = 0.81$.

It is known that an increase of the diameter of the holes on one side would raise the transparency of the grids resulting in a beneficial effect on the ion production cost, but in this case the perveance at which the optimal focusing of the beamlet is provided (the optimal perveance) is decreased. To resolve these contradictions, the string-type grid system may be used, in which every grid is formed by a system of parallel strings arranged in one plane. Strings are fastened to the mount ring by means of spring elements compensating for thermal deformations and providing stable operation of a grid system. By combined operation of the discharge chamber and the beam extraction system, whose grids were formed by tungsten strings with vertical separation of 1.5 mm at a diameter of 0.2 mm, the transparency was increased as high as 0.86. This resulted in a reduction in losses due to ion recombination on the screen grid surface. However, the high transparency promotes the output of neutral atoms from the discharge chamber. Therefore, effective ionization could be provided under high xenon flow rates. Hence, good results ($C_i = 350$ W/A and $\eta_g = 0.70$) were obtained for an ion beam current density of about 10 mA/cm^2. This points to the high perveance of the grid system because in this configuration the high transparency is combined with small absolute sizes of the elementary cell (a single set of apertures in the screen and accelerating grids); however, provision of long-term lifetime at such current densities is highly improbable considering the thickness of the accelerator grid.

Because of the results obtained, the string-type grid system assembly was newly constructed, where the screen grid was formed by 0.2-mm-diam strings and the accelerator grid was formed by

Table 1 Modes of the laboratory model ion thruster

Grid type	N, W	U_d, V	I_d, A	R, mN	U_s, V	U_a, V	I_b, mA	m, eq. mA	R_{sp}, s	C_i, W/A	η_g	η_e	η_t
Flat	52	44	0.3	1.8	1200	−1050	32	39	3400	370	0.81	0.77	0.62
String	39	46	0.2	1.6	1000	−300	30	39	2900	260	0.77	0.80	0.62

0.9-mm-diam strings (Fig. 2). Thus, the screen grid transparency remained high (0.86), resulting in a low ion recombination on its surface, while the transparency for the accelerator grid was reduced to 0.40, hindering the neutral atoms output from the discharge chamber, increasing a concentration thereof, and improving ionization conditions. Thus, at a flow rate of 39 eq. mA and a beam current of 30 mA, the ion production cost did not exceed 260 W/A at propellant utilization efficiency of 0.77.

The ion production cost as a function of the propellant utilization efficiency at a ion current of 30 mA is given in Fig. 4 (the lower curve). The screen grid was at 1000-V potential, the accelerator grid at −300 V. The propellant flow rate decreased from 59 eq. mA down to 39 eq. mA, and the discharge voltage varied within the limits from 36 to 46 V.

Typical operating characteristics of the laboratory-model ion thruster with the two types of grid systems are presented in Table 1.

The use of the string-type grid system allowed one to essentially reduce the accelerator grid potential as compared to the conventional grid system with flat grids. The reason is that the elementary cell of the string grid system has small sizes resulting in high optimal perveance.

The preceding results were obtained for the steadily operating heater of the hollow cathode. The power expended for its operation was not taken into account when calculating the ion production cost. Consequently, the relations obtained may be considered as a certain limiting case achievable after improvement of the cathode assembly so that it would operate in automode at discharge power less than 25–30 W.

All experiments were conducted without the neutralizer. One can estimate expenditures of power and propellant for operation of the neutralizer, using, for example, the information of Ref. 8, where the test results of ion engine subsystem for satellite ETS-VI are given. The neutralizer used in this thruster operates at 8.2-W power and a propellant flow rate of 40 eq. mA. For the thruster in question, the use of a neutralizer with such characteristics will result in a decrease of electrical efficiency from 0.77 down to 0.66 and the propellant utilization efficiency from 0.81 down to 0.46.

Conclusion

A 5-cm laboratory-model ion thruster with a design power ranging from 50 to 100 W was investigated. Applications of these thrusters include orbit correction propulsion systems for next-generation small-size and small-mass spacecraft. The efficiency of the thruster discharge chamber with a power consumption from 35 to 60 W (close to the lower limit of the design power range) was investigated. The operation of the model with the two types of grid systems was studied: the conventional grid system with flat perforated grids and the string-type system. It is shown the laboratory model developed provides ion beam generation with a beam current of about 30 mA with the following characteristics: 1) for the conventional beam-extraction system $C_i = 370$ W/A and $\eta_g = 0.81$ and 2) for the string-type grid system $C_i = 260$ W/A and $\eta_g = 0.77$.

This corresponds to a thrust from 1.5 to 2.0 mN. Efficient operation of the discharge chamber was realized at a discharge voltage of 38 V and more.

The use of the string grid system with small sizes of elementary cell in conjunction with the high transparency of the screen grid has allowed it to provide effective operation of the thruster at a low accelerator grid potential.

References

[1] Barnhart, D., Wojnar, R., Tilley, D., and Spores, R., "The Case for Small Spacecraft: An Integrated Perspective on Electric Propulsion," *Proceedings of the 24th International Electric Propulsion Conference*, Paper 95-148, Moscow, Russia, Sept. 1995.

[2] Fearn, D., and Wallace, N. C., "A Low Altitude Mapping Mission Using Ion Propulsion for Drag Compensation," *Proceedings of the Small Satellites for Remote Sensing. Space Congress*, Bremen, Germany, May 1995, pp. 41–53.

[3] Hyman, J., Jr., "Development of a 5-cm Flight-Qualified Mercury Ion Thruster," *Journal of Spacecraft and Rockets*, Vol. 10, No. 8, 1973, pp. 503–509.

[4] Herron, B. G., Hyman, J., Hopper, D. J., Williamson, W. S., Dulgeroff, C. R., and Collet, C. R., "Engineering Model 8-cm Thruster System," AIAA Paper 78-646, April 1978.

[5] Nakamura, Y., Miyazaki, K., and Suzuki, E., "Operation and Performances of a 5-cm Diameter Ion Thruster by Using Inert Gases," AIAA Paper 82-1924, 1982.

[6] Kaufman, H. R., "An Ion Rocket with an Electron-Bombardment Ion Source," NASA TN D-585, 1961.

[7] Wilbur, P. G., and Kaufman, H. R., "Double Ion Production in Argon and Xenon Ion Thrusters," *Journal of Spacecraft and Rockets*, Vol. 16, No. 4, 1979, pp. 264–267.

[8] Nagano, H., Kajiwara, K., Gotoh, Y., Nishida, E., and Fujita, Y., "On-Orbit Performance of ETS-VI Ion Engine Subsystem," *Proceedings of the 24th International Electric Propulsion Conference*, Paper 95-139, Moscow, Sept. 1995.